Rotational Stagnation Point Non-Newtonian Second-Grade Fluid Flowing over Spiraling Disk

Aamar Abbasi[1], Waseh Farooq[1], Fazle Mabood[2], Asma Tariq[1], Sabir Ali Shehzad[3,*], Irfan Anjum Badruddin[4]

[1]Department of Mathematics, University of Azad Jammu and Kashmir Muzaffarabad 13100, Pakistan

[2]Department of Information Technology, Fanshawe College London, ON Canada

[3]Department of Mathematics, COMSATS University Islamabad, Sahiwal 57000, Pakistan

[4]Department of Mechanical Engineering, College of Engineering, King Khalid University, Asir - Abha 61421, KSA

[*]Corresponding Author Email: ali_qau70@yahoo.com

Abstract

Numerical study is conducted to execute the analysis of rotational stagnation point second-grade liquid flowing over the spiraling rotatory disk. Heat transmission analysis is accounted. The problem is formulated in the coupled partial differential equations forms which are later simplified in view of similar variables. The Keller-Box (KB) procedure is adopted for the execution of numerical solutions. The involved parameters influences on the velocity and temperature profiles are presented and interpreted. The skin-frictions and Nusselt number are reported in the forms of numerical data. The present results are verified through the comparison with already available material in the literature. This study addressed that the thickness layer of boundary augmented against the incrementing viscoelastic and rotational parameters. Both rotational and viscoelasticity resist the temperature. The rotational parameter rises radial skin-friction and heat transmission rate while diminishes the swirl skin friction.

Keywords: Rotatory stagnation point; Second-grade fluid; Spiraling disk; Heat transfer; Keller-Box method

List of Symbols

T_∞	Ambient temperature	r	Radial coordinate
Ω	Angular velocity	C_{fr}	Radial skin friction
z	Axial coordinate	σ	Rotation rate parameter
$\tau_{f\phi}$	Azimuthal shear stresses	c_p	Specific heat
$C_{f\phi}$	Azimuthal skin friction	τ	Stress tensor
μ	Coefficient of viscosity	S	Suction/ injection parameter
α_2	Cross -viscosity of the fluid	T_w	Surface temperature
ρ	Density	T	Temperature
f,g	Dimensionless similarity variables	k	Thermal conductivity
θ	Dimensionless temperature	α	Thermal diffusivity
br	Disk stretching velocity	U,V,P,q,Y	Variables
q_w	Heat flux	u,v,w	Velocity components
A_1,A_2	Kinematic tensors	$\boldsymbol{V}$	Velocity field
ξ	Kinematic viscosity	α_1	Viscoelasticity
Pr	Prandtl number	We	Weissenberg number
τ_{wr}	Radial stress		

1. Introduction

The stagnation point flow investigation is concerned with the motion in surrounding the stagnation point of a rigid surface or moving fluid. Such flows have great physical significance because they forecast the heat transportation and skin-friction in the stagnation region. Due to wide applications of stagnation point flow, several theoretical investigations have been reported by the many researchers. Hiemenz [1] was probably first who analyzed the flow of viscous liquid impinging on infinitely long flat surface. Homann [2] deliberated the axisymmetric Newtonian liquid flow in the neighborhood of stagnation point over a flat surface. Hannah [3] extended this research by adopting the flow generation due to disk rotation. Weidman and Mahalingam [4] studied the axisymmetric flow of incompressible viscous fluid sticking on oscillating porous plate. Mahapatra and Gupta [5] discussed the

stagnation-point viscous liquid flowing over the linear stretched sheet. Lok et al. [6] addressed the Newtonian liquid flow in stagnation regime of a stretched sheet. Sajid et al. [7] numerically inspected the stagnant-point Newtonian liquid flow flowing over a power-law lubricant surface. The time-dependent stagnant point viscous liquid flowing over an impulsively rotating circular disk is executed by Hayat and Nawaz [8]. The above researchers adopted the Hiemenz and Homann flows of viscous fluid where the far field flow is irrotational. Turner and Weidman [9] studied the impingement axisymmetric stagnant point viscous material flow over a surface executed planar and perpendicular. Takhar et.al, [10] discussed the axisymmetric flow of fluid striking the surface circular cylinder. Mabood et al. [11] described the non-linear radiative influences in stagnation point Oldroyd-B nanomaterial flow. Mathew et al. [12] elucidated the magnetized stratification effects on stagnation point ferro-nanomaterial flow through response surface technique. Raman et al. [13] executed the multiple slip factors on magnetic stagnation point Casson material flow.

Heat transfer is a phenomena that transmits energy from one place to another and this phenomena is prevalent in our daily life and has ample applications in engineering like gas turbine, power plants, cooling of electronic machines and aircraft engine, thermal production of space shuttles, etc. The stagnation zone sensitizes that the heat transportation rate is maximum and the efficiency of cooling is strongly influenced due to numerous reasons. Motivated by such facts, several theoretical studies have been developed to address the energy transportation features in stagnant-point flows. Bhattacharyya et al. [14] examined the heat transmission nature in the stagnant-point neighborhood and reported that the rate of heat transmission reduced against the higher velocity rotation constraint. The axisymmetric heat transportation of compressible viscous liquid impinging on cylinder is illustrated by Mohammadiun et al. [15]. Dero et al. [16] discussed the electrically conducting water-based nanomaterial flow induced by the stagnant point exponential shrinked permeable surface.

Alizadeh et al. [17] deliberated the time-independent heat transmission of Newtonian fluid in non-axisymmetric stagnation point zone. Abbas et al. [18] addressed the heterogeneous-homogenous chemically reactive and magnetized Newtonian fluid flow near a stagnant-point. The energy transport analysis of three dimensional stagnation-point viscous liquid flowing in the zone of linear moving surface is examined by Rehman et al. [19]. Mabood and Khan [20] studied the heat transport behavior in Newtonian material flowing through the Darcy's porous space. Kamal et al. [21] elaborated the analysis of energy transport and liquid motion for Newtonian fluid flowing over the permeable disk and highlighted the heat source influences. Yasin et al. [22] examined the Newtonian heating, magnetic field, viscous dissipation, and partial slip influences on the energy transport characteristics of Newtonian fluid. Shateyi and Makinde [23] presented the heat and flow features behavior of viscous fluid impinging on a convective stretched disk. Khan et al. [24] numerically investigate the Darcy- Forchheimer flow of viscous fluid over a rotating disk incorporating the partial slip conditions. Chu et al. [25] illustrated the Newtonian nanofluid through porous space. Chu et al. [26] analyzed the influence of solid volume fractions and heat generation on the flow and thermal characteristics. Mustafa et al. [27] inspected the heat transportation in the boundary-driven ferrofluid flowing on a rotating disk. Roşca and Pop [28] addressed the rotational stagnation-point viscous material flow with normal impingement on a radially porous stretching surface. Abbasi et al. [29] numerically reported the thermally radiated activation energy influences on the rotational stagnant-point hybrid fluid flow. Farooq et al. [30] explore the rotational stagnation point flow of carbon nanotubes executed by bi-directional stretching sheet.

Motion of fluid attracts attention in many real-life problems such as wings of air crafts and oscillating bodies. Moreover, this phenomenon is well known for its applications in engineering and industries. Natural, industrial, and technological fluids that exhibit shear dependent viscosity cannot be analyzed through Navier-Stokes equations. To categorize the

rheology of such fluids, various models have been proposed. Viscoelastic fluid models is a paramount subclass of the differential type model of non-Newtonian fluid in which grade fluid proposed by Rivlin [31] is simple and it covers linear viscoelastic behavior that has broader range of implications in the polymer sector. Beard and Walters [32] addressed the elastico-viscous liquid flowing near the stagnation zoon and show that the viscoelasticity enhance the velocity in boundary layer region also stress on the solid boundary. Ariel [33] presented an algorithm for the numerical approximation of the formulated equations of two dimensional second-grade non-Newtonian liquid flowing over a circular disk. Baris and Dokuz [34] probed the flow of viscoelastic fluid over a moving surface. Labropulu et al. [35] highlighted the time dependent flow of viscoelastic fluid near a stagnation zoon. Analytic and numeric computations for non-Newtonian second grade material flow under viscous heating induced by the convected moving surface is illustrated by Bhuvaneswari et al. [36]. Krishna et al. [37] addressed the Ion and Hall flow of time-dependent rotatory second-grade liquid under convective heat absorption. Xia et al. [38] considered the Forchheimer-Darcy and Lorentz forces to describe the Couette-Taylor second-grade flow situation. Siddique et al. [39] discussed the time-dependent second grade model of fractional heat transportation. Mabood et al. [40] highlighted the effects of Newtonian heating, suction and mixed convection on the flow of second grade fluid. Chu et al. [41] simulate the hydromagnetized non-Newtonian fluid near stagnation point. Zhao et al. [42] reported the thermal transmission in the stagnation point flow of electrically conducting fluid. Furthermore, Abbas et al. [43], Yavuz [44], Nadeem et al. [45], Nisa et al. [46], Alamri et al. [47], Khan et al. [48], Saif et al. [49] and Tariq et al. [50] examined the different flows of second-grade fluid.

Owning the tremendous applications of stagnation point flows due to their importance in science and engineering like cooling of electronic devices, nuclear reactors metallic plate, and by fans, crystal puffing, plastic glass and films drawing continuous costing, production of

papers, food processing, wire drawing etc. and keeping the fact in mind that most of the industrial fluids are combination of dissimilar stuffs such as oil, water or a mixture of chain molecules, these fluids shows non-Newtonian behavior in the response of applied stresses Natural, industrial, and technological fluids that exhibit shear dependent viscosity cannot be analyzed through Navier-Stokes equations. To categorize the rheology of such fluids, the second-grade fluid model is simplest subclass of viscoelastic fluid models in this paper a numerical study is carried out to deliberate the rotational stagnation point flow of second-grade fluid over a circular spiraling disk. The governed physical equations are converted by the use of similarity constraints. This non-dimensional model is treated by the utilization of Keller-Box scheme. The graphical illustration and numerical benchmarks are produced to address and analyze the behavior of versatile involved parameters on physical quantities.

2. Problem Formulation

The axisymmetric movement of Rivlin-Erickson type fluid near rotational stagnant-point over spiraling disk. The disk is in rotation through the angular velocity Ω about $z-$axis. The disk is stretched in radial direction under velocity br (see Fig. 1). The model is reported in cylindrical coordinates r,ϕ and z with corresponding velocity components u,v and w respectively. Here, $z = 0$ represents the disk surface which maintained at temperature T_w and $z > 0$ is the space occupied by the fluid and the ambient temperature is assumed to be T_∞.

Fundamental conservation laws are utilized for the mathematical modeling of the problem. For an incompressible fluid the continuity equations is:

$$\nabla.\boldsymbol{V} = 0, \tag{1}$$

In the absence of body forces for steady axisymmetric incompressible liquid flow, the momentum equation in components form can be expressed as:

$$\rho\left[u\frac{\partial u}{\partial r}+w\frac{\partial u}{\partial z}-\frac{v^2}{r}\right]=-\frac{\partial p}{\partial r}+\frac{1}{r}\frac{\partial\left(r\tau_{rr}\right)}{\partial r}+\frac{\partial\left(\tau_{rz}\right)}{\partial z}-\frac{\tau_{\phi\phi}}{r}, \tag{2}$$

$$\rho\left[u\frac{\partial v}{\partial r}+w\frac{\partial v}{\partial z}-\frac{uv}{r}\right]=\frac{1}{r^2}\frac{\partial\left(r^2\tau_{\phi r}\right)}{\partial r}+\frac{\partial\left(\tau_{\phi z}\right)}{\partial z}-\frac{\tau_{\phi r}-\tau_{\phi r}}{r}, \tag{3}$$

$$\rho\left[u\frac{\partial w}{\partial r}+w\frac{\partial w}{\partial z}\right]=-\frac{\partial p}{\partial z}+\frac{1}{r}\frac{\partial\left(r\tau_{zr}\right)}{\partial r}+\frac{\partial\left(\tau_{zz}\right)}{\partial z}, \tag{4}$$

In above u,v,w are velocity components along radial azimuthal and axial direction, ρ is the density of the fluid $\tau_{rr},\tau_{\phi r},\tau_{rz},\tau_{\phi\phi},\tau_{\phi z}$ and τ_{zz} are the component of stress tensor τ. Most of the industrial fluid are non- Newtonian and have been modeled using relatively simple constitutive equation presented by Rivlin [31]:

$$\tau=-pI+\mu A_1+\alpha_1 A_2+\alpha_2 A_2^2, \tag{5}$$

In which p is pressure, A_1,A_2 are kinematic tensors, μ is coefficient of viscosity α_1 is viscoelasticity and α_2 is cross-viscosity of the fluid and for a second grade fluid theses constants satisfy the stable thermodynamic conditions defined by Dunn and Fosdick [51] as $\alpha_1\geq 0,\mu\geq 0$ and $\alpha_1+\alpha_2=0$. The energy balance equation in the absence of Joule and Ohmic dissipations has the following form:

$$\rho c_p\left(\frac{dT}{dt}\right)=k\nabla^2 T. \tag{6}$$

Where c_p is used to represent the specific heat, T and k denotes the temperature and thermal conductivity of the fluid. In view of Weidman [52] the pertinent boundary conditions satisfy by the velocity components along with the surface and ambient temperature conditions are

$$\begin{aligned} u = br, v = r\Omega, w = 0, T = T_w \quad & when \quad z \to 0, \\ u(r,z) = 2arz, w(r,z) = -2az^2, T = T_\infty \quad & when \quad z \to \infty. \end{aligned} \tag{7}$$

For incompressible axisymmetric second-grade liquid, the equations (1-5) can be expressed as:

$$\frac{u}{r} + \frac{\partial u}{\partial r} + \frac{\partial w}{\partial z} = 0, \tag{8}$$

$$\begin{aligned} u\frac{\partial u}{\partial r} + w\frac{\partial u}{\partial z} - \frac{v^2}{r} = -\frac{1}{\rho}\frac{\partial p}{\partial r} + \xi\left[2\frac{\partial^2 u}{\partial r^2} + \frac{\partial}{\partial z}\left(\frac{\partial u}{\partial z} + \frac{\partial w}{\partial r}\right) + \frac{2}{r}\frac{\partial u}{\partial r} - \frac{2u}{r^2}\right] + \frac{\alpha_1}{\rho}\left\{2\frac{\partial}{\partial r}\left(u\frac{\partial^2 u}{\partial r^2}\right) - \right. \\ \frac{\partial}{\partial r}\left(\frac{\partial u}{\partial z}\right)^2 + \frac{\partial}{\partial r}\left(\frac{\partial v}{\partial r}\right)^2 + 2\frac{\partial}{\partial r}\left(w\frac{\partial^2 u}{\partial z \partial r}\right) - \frac{\partial}{\partial r}\left(\frac{v^2}{r^2}\right) + \frac{\partial}{\partial r}\left(\frac{\partial w}{\partial r}\right)^2 + \frac{\partial}{\partial z}\left(u\frac{\partial^2 u}{\partial r \partial z}\right) + \frac{\partial}{\partial z}\left(u\frac{\partial^2 w}{\partial r^2}\right) + \\ \frac{\partial}{\partial z}\left(w\frac{\partial^2 u}{\partial z^2}\right) + \frac{\partial}{\partial z}\left(\frac{\partial u}{\partial z}\frac{\partial u}{\partial r} - \frac{\partial w}{\partial r}\frac{\partial u}{\partial r} + \frac{\partial w}{\partial r}\frac{\partial w}{\partial z} + \frac{\partial v}{\partial r}\frac{\partial v}{\partial z} - \frac{\partial u}{\partial z}\frac{\partial w}{\partial z} + w\frac{\partial^2 w}{\partial z \partial r}\right) + \frac{2u}{r}\frac{\partial^2 u}{\partial r^2} + \frac{2w}{r}\frac{\partial^2 u}{\partial z \partial r} \\ \left. - \frac{2u}{r^2}\frac{\partial u}{\partial r} - \frac{2w}{r^2}\frac{\partial u}{\partial z} + \frac{2}{r}\left(\frac{\partial v}{\partial r}\right)^2 + \frac{1}{r}\left(\frac{\partial w}{\partial r}\right)^2 - \frac{1}{r}\left(\frac{\partial u}{\partial z}\right)^2 + \frac{1}{r}\left(\frac{\partial v}{\partial z}\right)^2 - \frac{2v^2}{r^3} + \frac{2u^2}{r^3}\right\}, \end{aligned} \tag{9}$$

$$\begin{aligned} u\frac{\partial v}{\partial r} + w\frac{\partial v}{\partial z} + \frac{uv}{r} = \xi\left[\frac{\partial^2 v}{\partial z^2} + \frac{\partial}{\partial r}\left(\frac{\partial v}{\partial r} - \frac{v}{r}\right) + \frac{1}{r}\frac{\partial v}{\partial r} - \frac{v}{r^2}\right] + \frac{\alpha_1}{\rho}\left\{\frac{\partial}{\partial r}\left(u\frac{\partial^2 v}{\partial r^2}\right) - \frac{\partial}{\partial r}\left(\frac{\partial v}{\partial r}\frac{\partial u}{\partial r}\right) - \right. \\ \frac{\partial}{\partial r}\left(\frac{\partial u}{\partial r}\frac{v}{r}\right) - \frac{\partial}{\partial r}\left(\frac{\partial u}{\partial z}\frac{\partial v}{\partial z}\right) + \frac{\partial}{\partial r}\left(w\frac{\partial^2 v}{\partial z \partial r}\right) - \frac{\partial}{\partial r}\left(\frac{w}{r}\frac{\partial v}{\partial z}\right) + \frac{\partial}{\partial r}\left(\frac{2uv}{r^2}\right) + \frac{\partial}{\partial z}\left(u\frac{\partial^2 v}{\partial r \partial z}\right) + \\ \frac{\partial}{\partial z}\left(w\frac{\partial^2 v}{\partial z^2}\right) - \frac{\partial}{\partial z}\left(\frac{\partial^2 u}{\partial z^2}\frac{v}{r}\right) - \frac{\partial}{\partial z}\left(\frac{\partial w}{\partial z}\frac{\partial v}{\partial z}\right) + \frac{\partial}{\partial z}\left(\frac{u}{r}\frac{\partial v}{\partial z}\right) - \frac{\partial}{\partial z}\left(\frac{\partial w}{\partial r}\frac{\partial v}{\partial r}\right) + \frac{u}{r}\frac{\partial^2 v}{\partial r^2} - \frac{\partial u}{\partial r}\frac{v}{r^2} \\ \left. - \frac{1}{r}\frac{\partial v}{\partial r}\frac{\partial u}{\partial r} - \frac{1}{r}\frac{\partial v}{\partial z}\frac{\partial u}{\partial z} + \frac{w}{r}\frac{\partial^2 v}{\partial z \partial r} - \frac{w}{r^2}\frac{\partial v}{\partial z} + \frac{2uv}{r^3}\right\}, \end{aligned} \tag{10}$$

$$\begin{aligned} u\frac{\partial w}{\partial r} + w\frac{\partial w}{\partial z} - \frac{v^2}{r} = -\frac{1}{\rho}\frac{\partial p}{\partial z} + \xi\left[2\frac{\partial^2 w}{\partial r^2} + \frac{\partial}{\partial r}\left(\frac{\partial u}{\partial z} + \frac{\partial w}{\partial r}\right) + \frac{1}{r}\frac{\partial u}{\partial z} + \frac{1}{r}\frac{\partial w}{\partial r}\right] + \frac{\alpha_1}{\rho}\left\{\frac{\partial}{\partial r}\left(u\frac{\partial^2 u}{\partial r \partial z}\right)\right. \\ + \frac{\partial}{\partial r}\left(u\frac{\partial^2 w}{\partial r^2}\right) + \frac{\partial}{\partial r}\left(w\frac{\partial^2 u}{\partial z^2}\right) + \frac{\partial}{\partial r}\left(w\frac{\partial w u}{\partial z \partial r}\right) + \frac{\partial}{\partial r}\left(\frac{\partial u}{\partial z}\frac{\partial u}{\partial r}\right) - \frac{\partial}{\partial r}\left(\frac{\partial w}{\partial z}\frac{\partial u}{\partial z}\right) + \frac{\partial}{\partial r}\left(\frac{\partial w}{\partial z}\frac{\partial w}{\partial r}\right) + \\ \frac{\partial}{\partial r}\left(\frac{\partial v}{\partial r}\frac{\partial v}{\partial z}\right) - \frac{\partial}{\partial r}\left(\frac{\partial w}{\partial r}\frac{\partial u}{\partial r}\right) + 2\frac{\partial}{\partial r}\left(\frac{\partial^2 w}{\partial z^2}w\right) + \frac{\partial}{\partial z}\left(\frac{\partial u}{\partial z}\right)^2 + \frac{\partial}{\partial z}\left(\frac{\partial v}{\partial z}\right)^2 - \frac{\partial}{\partial z}\left(\frac{\partial w}{\partial r}\right)^2 + \frac{w}{r}\frac{\partial^2 u}{\partial z^2} \\ \left. + 2\frac{\partial}{\partial z}\left(u\frac{\partial^2 w}{\partial z \partial r}\right) + \frac{u}{r}\left(\frac{\partial^2 u}{\partial r \partial z} + \frac{\partial^2 w}{\partial r^2}\right) + \frac{1}{r}\left(\frac{\partial v}{\partial z}\frac{\partial v}{\partial r} + \frac{\partial w}{\partial z}\frac{\partial w}{\partial r} - \frac{\partial w}{\partial z}\frac{\partial u}{\partial z} + \frac{\partial u}{\partial z}\frac{\partial u}{\partial r} - \frac{\partial w}{\partial r}\frac{\partial u}{\partial r}\right)\right\}, \end{aligned} \tag{11}$$

$$u\frac{\partial T}{\partial r}+w\frac{\partial T}{\partial z}=\alpha\left[\frac{\partial^2 T}{\partial r^2}+\frac{1}{r}\frac{\partial T}{\partial r}+\frac{\partial^2 T}{\partial z^2}\right], \tag{12}$$

In which $\xi=\mu/\rho$ represents kinematic viscosity and $\alpha=k/c_p$ is the thermal diffusivity. In all above cited literature about second grade fluid the similarity variables for which the far field flow is irrotational. Weidman [52] suggested that the similarity variables which give rise the rotational stagnation point in the obey the mass conservation law are provided as below

$$u(r,\eta)=a^{2/3}r\xi^{1/3}f'(\eta), v(r,\eta)=rg(\eta)\Omega, w(\eta)=-2a^{1/3}r\xi^{2/3}g(\eta), \tag{13}$$

Where $\eta=\left(\frac{a}{\xi}\right)^{1/2}z$, a is constant. The temperature equation can be transformed by introducing $T=\theta(\eta)(T_w-T_\infty)+T_\infty$. By invoking the above similarity constraints, the continuity is automatically satisfied and pair of differential equations is obtained for second grade fluid which along with energy equation takes the form

$$f'''-f'^2+2ff''+\sigma^2g^2+We\left(f''^2+2f'f'''-2ff^{iv}+\sigma^2\left(g'^2+gg''\right)\right)=0, \tag{14}$$

$$g''+2\left(fg'-f'g\right)+We\left(2f'g''-2fg'''-f'''g\right)=0, \tag{15}$$

$$\theta''+2Pr\ f\theta'=0. \qquad 1 \tag{16}$$

The non-dimensional conditions are:

$$f(\eta)=S, f'(\eta)=\beta, g(\eta)=1=\theta(\eta) \quad when \quad \eta\to 0, \tag{17}$$

$$f''(\eta)=2, f'''(\eta)=0, g(\eta)=0=g'(\eta)=\theta(\eta) \quad when \quad \eta\to\infty. \tag{18}$$

In above over prime is the derivative with respect to the η. The dimensionless numbers $We=\alpha_1 a^{2/3}/\rho\xi^{2/3}$ depicts the Weissenberg number, $\sigma=\Omega/a^{2/3}\xi^{1/3}$ is dimensionless rotation rate

parameter, $Pr = \xi / \alpha$ is Prandtl number, β is stretching parameter and S is suction/ injection parameter. The skin friction coefficients along radial and azimuthal directions are expressed as

$$C_{fr} = \frac{\tau_{wr}\big|_{z=0}}{\rho U_W^2}, \quad C_{f\phi} = \frac{\tau_{w\phi}\big|_{z=0}}{\rho(r\Omega)^2} \tag{19}$$

Elucidation of wall shear stresses τ_{wr} and $\tau_{w\phi}$ along radial and azimuthal directions are

Skin friction coefficients in dimensionless form are given as

$$\sqrt{Re}C_{fr} = \left[f'' + We\left(4f'\,f'' - 2ff''' + \sigma^2 gg'\right)\right]_{\eta=0}, \tag{20}$$

$$\sqrt{Re_r}C_{f\phi} = \left[g' + We\left(4f'g' - 2ffg'' - f''g\right)\right]_{\eta=0} \tag{21}$$

where $\sqrt{Re}$ and $\sqrt{Re_r}$ are the local and rotating Reynold numbers.

Heat transfer rate by Fourier law of conduction at the surface of disk is

$$q_w = -k\left(\frac{\partial T}{\partial z}\right)_{z=0},$$

3. Solution methodology

The transformed equations (14-16) subject to conditions (17-18) are approximated numerically by employing finite difference method which is commonly titled by Keller box method in literature. The whole numerical procedure is implemented in four steps.

Step 1: Reducing the equations (14-16) into first order system of equations. For this let

$$f' = U, U' = V, V' = W, g' = P, P' = q, \theta' = Y, \tag{22}$$

we get

$$V'-U^2+2fV+\sigma^2g^2+We\left(V^2+2UW-2fW'+\sigma^2P^2+\sigma^2qg\right)=0, \tag{23}$$

$$P'+2\left(fP-Ug\right)+We\left(2Uq-2fq'-Wg\right)=0, \tag{24}$$

$$Y'+2Pr\ fY=0. \tag{25}$$

The associated boundary conditions are

$$f(\eta)=S,U(\eta)=\beta,g(\eta)=1=\theta(\eta) \quad when \quad \eta\to 0, \tag{26}$$

$$V(\eta)=2,W(\eta)=0,g(\eta)=0=P(\eta)=\theta(\eta) \quad when \quad \eta\to\infty. \tag{27}$$

Step 2: Computing the derivative by centered difference and rest of dependent variables by taking averaging at the midpoint of the net. The derivatives are approximated by the relation $\eta_{0,}=0,\eta_j=\eta_{j-1}+h_j, j=1,2,3,.....,J,\eta_J=\eta_\infty$. So the equations (22-25) takes the form

$$\left.\begin{aligned}
&\frac{f_j-f_{j-1}}{h_j}=U_{j-\frac{1}{2}}\\
&\frac{U_j-U_{j-1}}{h_j}=V_{j-\frac{1}{2}}\\
&\frac{V_j-V_{j-1}}{h_j}=W_{j-\frac{1}{2}}\\
&\frac{g_j-g_{j-1}}{h_j}=P_{j-\frac{1}{2}}\\
&\frac{P_j-P_{j-1}}{h_j}=q_{j-\frac{1}{2}}\\
&\frac{\theta_j-\theta_{j-1}}{h_j}=Y_{j-\frac{1}{2}}
\end{aligned}\right\}, \tag{28}$$

$$\begin{aligned}
&\frac{V_j-V_{j-1}}{h_j}-U^2_{j-\frac{1}{2}}+2f_{j-\frac{1}{2}}V_{j-\frac{1}{2}}+\sigma^2g^2_{j-\frac{1}{2}}\\
&+We\left(V^2_{j-\frac{1}{2}}+2U_{j-\frac{1}{2}}V_{j-\frac{1}{2}}-2f_{j-\frac{1}{2}}\frac{W_j-W_{j-1}}{h_j}+\sigma^2P^2_{j-\frac{1}{2}}+\sigma^2g_{j-\frac{1}{2}}q_{j-\frac{1}{2}}\right)=0,
\end{aligned} \tag{29}$$

$$\frac{P_j - P_{j-1}}{h_j} + 2\left(f_{j-\frac{1}{2}} P_{j-\frac{1}{2}} - U_{j-\frac{1}{2}} g_{j-\frac{1}{2}} \right) + We\left(2U_{j-\frac{1}{2}} q_{j-\frac{1}{2}} - 2 f_{j-\frac{1}{2}} \frac{q_j - q_{j-1}}{h_j} - W_{j-\frac{1}{2}} g_{j-\frac{1}{2}} \right) = 0, \tag{30}$$

$$\frac{Y_j - Y_{j-1}}{h_j} + 2\,Pr\, f_{j-\frac{1}{2}} Y_{j-\frac{1}{2}} = 0. \tag{31}$$

where $f_{j-\frac{1}{2}} = \frac{f_j + f_{j-1}}{2}$ etc.

Step 3: Equations (28)-(31) are non-linear before factorization we apply the Newton's method for which we write the Newton's iterates as follows: For the $(i+1)th$, iterates, we write $f_j^{i+1} = f_j^i + \delta f_j^i$, for all dependent variables. After using the above procedure of linearization, we write the linear tri-diagonal system of algebraic equations as follows:

$$\delta f_j - \delta f_{j-1} - \frac{h_j}{2}\left(\delta U_j + \delta U_{j-1}\right) = \left(r_1\right)_{j-\frac{1}{2}}, \tag{32}$$

$$\delta g_j - \delta g_{j-1} - \frac{h_j}{2}\left(\delta P_j + \delta P_{j-1}\right) = \left(r_2\right)_{j-\frac{1}{2}}, \tag{33}$$

$$\xi_1\delta f_j + \xi_2\delta f_{j-1} + \xi_3\delta U_j + \xi_4\delta U_{j-1} + \xi_5\delta V_j + \xi_6\delta V_{j-1} + \xi_7\delta W_j + \xi_8\delta W_{j-1} + \xi_9\delta g_j + \xi_{10}\delta g_{j-1} + \xi_{11}\delta P_j + \xi_{12}\delta P_{j-1} + \xi_{13}\delta q_j + \xi_{14}\delta q_{j-1} = \left(r_3\right)_{j-\frac{1}{2}}, \tag{34}$$

$$\psi_1\delta f_j + \psi_2\delta f_{j-1} + \psi_3\delta U_j + \psi_4\delta U_{j-1} + \psi_5\delta W_j + \psi_6\delta W_{j-1} + \psi_7\delta g_j + \psi_8\delta g_{j-1} + \psi_9\delta P_j + \psi_{10}\delta P_{j-1} + \psi_{11}\delta q_j + \psi_{12}\delta q_{j-1} = \left(r_4\right)_{j-\frac{1}{2}}, \tag{35}$$

$$\lambda_1\delta f_j + \lambda_2\delta f_{j-1} + \lambda_3\delta Y_j + \lambda_4\delta Y_{j-1} == \left(r_5\right)_{j-\frac{1}{2}}, \tag{36}$$

$$\delta U_j - \delta U_{j-1} - \frac{h_j}{2}\left(\delta V_j + \delta V_{j-1}\right) = \left(r_6\right)_{j-\frac{1}{2}}, \tag{37}$$

$$\delta V_j - \delta V_{j-1} - \frac{h_j}{2}\left(\delta W_j + \delta W_{j-1}\right) = \left(r_7\right)_{j-\frac{1}{2}}, \tag{38}$$

$$\delta P_j - \delta P_{j-1} - \frac{h_j}{2}\left(\delta q_j + \delta q_{j-1}\right) = \left(r_8\right)_{j-\frac{1}{2}}, \tag{39}$$

$$\delta\theta_j - \delta\theta_{j-1} - \frac{h_j}{2}\left(\delta Y_j + \delta Y_{j-1}\right) = \left(r_9\right)_{j-\frac{1}{2}}, \tag{40}$$

where

$$\xi_1 = \frac{h_j}{2} V_{j-\frac{1}{2}} - We\left(W_j - W_{j-1}\right) \quad \xi_2 = \xi_1, \quad \xi_3 = -h_j U_{j-\frac{1}{2}} + Weh_j W_{j-\frac{1}{2}} \quad \xi_4 = \xi_3$$

$$\xi_5 = 1 + \frac{h_j}{2} f_{j-\frac{1}{2}} + Weh_j V_{j-\frac{1}{2}} \quad \xi_6 = -1 + \frac{h_j}{2} f_{j-\frac{1}{2}} + Weh_j V_{j-\frac{1}{2}}$$

$$\xi_7 = Weh_j U_{j-\frac{1}{2}} - 2Wef_{j-\frac{1}{2}} \quad \xi_8 = Weh_j U_{j-\frac{1}{2}} - 2Wef_{j-\frac{1}{2}}$$

$$\xi_9 = h_j \sigma^2 g_{j-\frac{1}{2}} + We\sigma^2 \frac{h_j}{2} q_{j-\frac{1}{2}} \quad \xi_{10} = \xi_9, \quad \xi_{11} = We\sigma^2 h_j P_{j-\frac{1}{2}} \quad \xi_{12} = \xi_{11}$$

$$\xi_{13} = We\sigma^2 h_j g_{j-\frac{1}{2}} \quad \xi_{14} = We\sigma^2 h_j g_{j-\frac{1}{2}}$$

$$\psi_1 = \frac{h_j}{2} P_{j-\frac{1}{2}} - We\left(q_j - q_{j-1}\right) \quad \psi_2 = \psi_1, \quad \psi_3 = -h_j g_{j-\frac{1}{2}} + Weh_j q_{j-\frac{1}{2}} \quad \psi_4 = \psi_3$$

$$\psi_5 = -We\frac{h_j}{2} g_{j-\frac{1}{2}} \quad \psi_6 = \psi_5, \quad \psi_7 = -We\frac{h_j}{2} W_{j-\frac{1}{2}} - h_j U_{j-\frac{1}{2}} \quad \psi_8 = \psi_7$$

$$\psi_9 = 1 + h_j f_{j-\frac{1}{2}} \quad \psi_{10} = -1 + h_j f_{j-\frac{1}{2}}$$

$$\psi_{11} = Weh_j U_{j-\frac{1}{2}} - 2Wef_{j-\frac{1}{2}} \quad \psi_{12} = Weh_j U_{j-\frac{1}{2}} + 2Wef_{j-\frac{1}{2}}$$

$$\lambda_1 = Pr\, h_j Y_{j-\frac{1}{2}} \quad \lambda_2 = \lambda_1, \quad \lambda_3 = 1 + Pr\, h_j f_{j-\frac{1}{2}} \quad \lambda_4 = -1 + Pr\, h_j f_{j-\frac{1}{2}}$$

Also

$$(r_1)_{j-\frac{1}{2}} = f_{j-1} - f_j + \frac{h_j}{2}(U_j + U_{j-1}),$$
$$(r_2)_{j-\frac{1}{2}} = g_{j-1} - g_j + \frac{h_j}{2}(P_j + P_{j-1}),$$

$$(r_3)_{j-\frac{1}{2}} = \begin{pmatrix} V_{j-1} - V_j + h_j U^2{}_{j-\frac{1}{2}} \\ -h_j f_{j-\frac{1}{2}} V_{j-\frac{1}{2}} - h_j \sigma^2 g^2{}_{j-\frac{1}{2}} \end{pmatrix} + We \begin{pmatrix} -h_j \sigma^2 P^2{}_{j-\frac{1}{2}} V^2{}_{j-\frac{1}{2}} - 2h_j U_{j-\frac{1}{2}} W_{j-\frac{1}{2}} + \\ 2 f_{j-\frac{1}{2}} (W_j - W_{j-1}) - h_j \sigma^2 g_{j-\frac{1}{2}} q_{j-\frac{1}{2}} \end{pmatrix},$$

$$(r_4)_{j-\frac{1}{2}} = \begin{pmatrix} q_{j-1} - q_j - 2h_j f_{j-\frac{1}{2}} p_{j-\frac{1}{2}} \\ + 2h_j g_{j-\frac{1}{2}} U_{j-\frac{1}{2}} \end{pmatrix} + We \begin{pmatrix} -2h_j U_{j-\frac{1}{2}} q_{j-\frac{1}{2}} + h_j W_{j-\frac{1}{2}} g_{j-\frac{1}{2}} + \\ 2 f_{j-\frac{1}{2}} (q_j - q_{j-1}) \end{pmatrix},$$

$$(r_5)_{j-\frac{1}{2}} = Y_{j-1} - Y_j - 2h_j \, Pr \, f_{j-\frac{1}{2}} Y_{j-\frac{1}{2}},$$

$$(r_6)_{j-\frac{1}{2}} = U_{j-1} - U_j + \frac{h_j}{2}(V_j + V_{j-1}),$$
$$(r_7)_{j-\frac{1}{2}} = V_{j-1} - V_j + \frac{h_j}{2}(W_j + W_{j-1}),$$
$$(r_8)_{j-\frac{1}{2}} = P_{j-1} - P_j + \frac{h_j}{2}(q_j + q_{j-1}),$$
$$(r_9)_{j-\frac{1}{2}} = \theta_{j-1} - \theta_j + \frac{h_j}{2}(q_j + q_{j-1}),$$

Step 04: After writing the equation (32-40) in matrix form having the block elements of 9×9 matrices, which are computed by block-tridiagonal elimination technique which consists of forward and backward sweeps.

4. Validation of Numerical Results

Table 1 provides the convergence of $f''(0), g''(0)$ and $-\theta'(0)$ at multiple grid points by fixing $We = 0.1, \sigma = 1.0, Pr = 4.0, S = 0.1$ and $\beta = 0.0$. In order to validate the present numerical scheme we compare the results of $f''(0)$ and $g'(0)$ for viscous fluid on a rigid rotating disk (see Table 2). The deep analysis of the results show that the results obtained by finite difference show a good agreement 3 to 4 decimal places.

5. Results and Discussion

The variation of radial velocity $f'(\eta)$ against the rheological parameter We, for several values of stretching parameter is examined in Fig. 2. The rheological parameter which demonstrates the viscoelasticity of the fluid reduces the radial velocity $f'(\eta)$ of the fluid for rising values of stretching parameter. Furthermore, when only rotating disk is considered the decline in velocity is large on the surface of the disk and when stretching of the disk is involved, the decline in velocity decreases and it is observed that the effects of viscoelasticity dismissed for large stretching of the disk. In many industrial process where the speed of the transporting fluids needs to be improved stretching is an important factor. The rise in Azimuthal velocity against viscoelasticity of the fluid for the different values of β is observed in Fig. 3. Also, it is noted that the velocity profile of the non-Newtonian fluid has maximum amplitude over rotating disk and it declines over stretching disk. Figs. 4-5 are plotted to computes the effects of rotation parameter σ on radial velocity $f'(\eta)$ and Azimuthal velocity $g(\eta)$ for various values of stretching parameter β. The rise in radial velocity $f'(\eta)$is noted against the incrementing rotation constraint. It is noted that rise is minimum corresponding to the rotation parameter over only rotating disk and rising rate is maximum as stretching of the disk is enhanced. The similar response is for radial velocity is reported by Weidman [52] for the Agarwal stagnation point flow of Newtonian fluid over rotating disk. The rotation parameter σ rises the azimuthal velocity of the viscoelastic fluid over both stretching and stationary disk. Figs. 6-7 displayed similarity velocities $f'(\eta)$ and $g(\eta)$ for both suction $(S = 0.1, 0.4)$ and blowing $(S = -0.1, -0.4)$ cases. The flow behavior is also analyzed for several values of stretching parameter β. The decreasing trend is followed for blowing case and the decreasing trend is boosted with rising the stretching velocity of the rotating disk. On the other hand, increasing trend is noted for the suction case and increasing behavior is

also improved with stretching of disk. The similar response for radial velocity is reported by Weidman [52] analyzing the rotational stagnation point flow over a radial stretching sheet with suction and blowing effects. The swirl velocity $g(\eta)$ show a similar response for both suction and blowing flow cases as radial velocity but the difference is that the increasing and decreasing behavior of velocity w.r.t blowing and suction minimizes with the stretching of disk. The decline in magnitude of swirl velocity occur with stretching parameter is probably due to rushing of fluid in radial direction.

Fig. 8 exhibits the decline in similarity temperature profile against the variation of viscoelastic parameter We for both $\beta = 0$ and $\beta > 0$. The decline in temperature of the fluid over rotatory disk is maximum and it cut off as stretching is involved. The temperature of the viscoelastic fluid also shows fall for several values of β in Fig. 9. It is observed that over non-rotating disk the rotation declines the temperature at large scale and fall in temperature reduces as stretching is involved. Fig. 10 reflects the Prandtl number Pr nature on temperature of the viscoelastic fluid over stretching and non-stretching disk. The decline in temperature against Prandtl number Pr is noted due to the fact that Prandtl number rises the heat transfer rate which cools the rotational system and as a result the decline in temperature inside the thermal boundary layer is noticed.

In Tables 3 and 4, the radial and swirl skin frictions are computed and presented for various values of rotation parameter σ and stretching parameter for both viscous and viscoelastic fluid. The rotation parameter rises the radial skin friction for viscous as well as non-Newtonian fluid. The rise is reliable with the fact that the viscoelastic boundary layer become thinner in radial direction with boosting rotation. The swirl or azimuthal skin friction is decreasing function of rotation parameter. The decreasing behavior is followed by swirl skin friction for viscous fluid $We = 0$ and decline is strengthen for viscoelastic fluid. Under the

influence of rotation the azimuthal boundary layer in viscoelastic fluid becomes thicker and as a result the azimuthal skin friction decreases. Both radial and azimuthal skin frictions are decreasing function of radial stretching parameter of the disk for several values of We. The stretching of the disk in radial direction thinner the viscoelastic boundary layer in both radial and azimuthal directions and as a result the corresponding shear stresses reduces. Furthermore, under the influence of strong rheology, radial skin friction has small magnitude with strong rotation and opposite trend is noted for azimuthal skin fraction with strong rotation.

The variation of Nusselt's number against the rotation parameter σ and stretching parameter β can be seen in table 5 for various values of We. Numerical values of Nusselt's number rises against rotation parameter for viscous fluid $We = 0$ and viscoelastic fluid $We > 0$. Similar trend is noted for Nusselt's number against the stretching parameter for both viscous and viscoelastic fluid. Furthermore, heat transfer rate increases with viscoelastic parameter We, because for higher values of viscoelastic parameter We the rotating fluid over a stretching disk has lower thermal conductivity, which overcomes the conduction and therefore rises the variation in heat transfer rate. Due to this reason, the reduction in thermal boundary layer thickness and rise in heat transfer rate over a spiraling disk is examined.

6. Conclusions

Numerical analysis is made to express the rotational stagnation point second-grade liquid flowing over the spiraling rotatory disk. The problem is formulated in the coupled partial differential equations forms which are later simplified in view of similar variables. The Keller-Box (KB) procedure is implemented for the numerical solutions of physical model.

Below are the final remarks of this conducted research:

- Both viscoelastic parameter and rotation parameter increase the radial and azimuthal boundary-layer thicknesses.
- The impact of viscoelastic parameter and rotation parameter are strengthened with the stretching of the disk.
- The radial and azimuthal velocities decline for blowing case and suction case.
- The temperature profile is decreasing function of rotation parameter, viscoelastic parameter and Prandtl number.
- The rotation parameter rises the radial skin friction while reduces the swirl skin friction.
- Both rotation and stretching parameters growth the heat transfer rate over spiraling disk.

Acknowledgment

The authors extend their appreciation to the Deanship of Scientific Research at King Khalid University for funding this work through the Large Groups Project under grant number RGP. 2/196/44.

Conflicts of Interest

The authors declare that there is no conflict of interest.

Authors Contributions

All authors contributed equally in this work.

References

1. Hiemenz, K. "Die Grenzschicht an einem in den gleichformigen Flussigkeitsstrom eingetauchten geraden Kreiszylinder", *Dingler's Polytechnical Journal*, **326**, pp. 321-324 (1911).

2. Homann, F. “Der Einfluss grosser Zähigkeit bei der Strömung um den Zylinder und um die Kugel”, *ZAMM- Journal of Applied Mathematics and Mechanics/Zeitschrift für Angewandte Mathematik und Mechanik,* **16**(3), pp. 153-164 (1936).
3. Hannah, D.M. “Forced flow against a rotating disk”, *Aeronautical Research Council Reports & Memoranda, London,* No. 2772, (1947).
4. Weidman, P.D., and Mahalingam, S. “Axisymmetric stagnation-point flow impinging on a transversely oscillating plate with suction”, *Journal of Engineering Mathematics,* **31**, pp. 305-318 (1997).
5. Mahapatra, T.R., and Gupta, A.S. “Stagnation- point flow towards a stretching surface”, *The Canadian Journal of Chemical Engineering,* **81**(2), pp. 258-263 (2003).
6. Lok, Y.Y., Ishak, A., and Pop, I. “MHD stagnation- point flow towards a shrinking sheet”, *International Journal of Numerical Methods for Heat & Fluid Flow,* **21**(1), pp. 61-72 (2011).
7. Sajid, M., Mahmood, K., and Abbas, Z. “Axisymmetric stagnation-point flow with a general slip boundary condition over a lubricated surface”, *Chinese Physics Letters,* **29**(2), 024702 (2012).
8. Hayat, T., and Nawaz, M. “Unsteady stagnation point flow of viscous fluid caused by an impulsively rotating disk”, *Journal of the Taiwan Institute of Chemical Engineers,* **42**(1), pp. 41-49 (2011).
9. Turner, M.R., and Weidman, P. “Homann stagnation-point flow impinging on a biaxially stretching surface”, *European Journal of Mechanics-B/Fluids,* **86**, pp. 49-56 (2021).
10. Takhar, H.S., Chamkha, A.J., and Nath, G. “Unsteady axisymmetric stagnation-point flow of a viscous fluid on a cylinder”, *International Journal of Engineering Science,* **37**(15), pp. 1943-1957 (1999).

11. Mabood, F., Abbasi, A., Farooq, W., et al. “Effects of non-linear radiation and chemical reaction on Oldroyd-B nanofluid near oblique stagnation point flow”, *Chinese Journal of Physics,* **77**, pp. 1197-1208 (2022).
12. Mathew, A., Areekara, S., and Sabu, A.S. “Significance of magnetic field and stratification effects on the bioconvective stagnation-point flow of ferro-nanofluid over a rotating stretchable disk: Four-factor response surface methodology”, *Journal of the Indian Chemical Society,* **99**, Article ID 100615 (2022).
13. Raman, R.M., Raju, K.V., and Kumar, J.G. “Multiple slips and heat source effects on MHD stagnation point flow of Casson fluid over a stretching sheet in the presence of chemical reaction”, *Materials Today: Proceedings,* **49**(5), pp. 2306-2315 (2022).
14. Bhattacharyya, K., Mukhopadhyay, S., and Layek, G.C. “Slip effects on boundary layer stagnation-point flow and heat transfer towards a shrinking sheet”, *International Journal of Heat and Mass Transfer*, **54**(1-3), pp. 308-313, (2011).
15. Mohammadiun, H., Rahimi, A. B., and Kianifar, A. “Axisymmetric stagnation-point flow and heat transfer of a viscous, compressible fluid on a cylinder with constant heat flux”, *Scientia Iranica,* **20**(1), pp. 185-194 (2013).
16. Dero, S., Abdelhameed, T.N., Al-Khaled, K., et al. “Contribution of suction phenomenon and thermal slip effects for radiated hybrid nanoparticles *(Al_2O_3-Cu/H_2O)* with stability framework”, *International Journal of Modern Physics B,* **37**(15), Article ID 2350147 (2022).
17. Alizadeh, R., Rahimi, A. B., and Najafi, M. “Non-axisymmetric stagnation-point flow and heat transfer of a viscous liquid on a stationary cylinder”, *Scientia Iranica*, **23**(5), pp. 2238-2246 (2016).
18. Abbas, Z., Sheikh, M., and Pop, I. “Stagnation-point flow of a hydromagnetic viscous fluid over stretching/shrinking sheet with generalized slip condition in the presence of

homogeneous–heterogeneous reactions", *Journal of the Taiwan Institute of Chemical Engineers,* **55**, pp. 69-75 (2015).

19. Rehman, F.U., Nadeem, S., and Haq, R.U. "Heat transfer analysis for three-dimensional stagnation-point flow over an exponentially stretching surface", *Chinese Journal of Physics,* **55**(4), pp. 1552-1560 (2017).
20. Mabood, F., and Khan, W.A. "Approximate analytic solutions for influence of heat transfer on MHD stagnation point flow in porous medium", *Computers & Fluids,* **100**, pp. 72-78 (2014).
21. Kamal, F., Zaimi, K., Ishak, A. et al. "Stability analysis on the stagnation-point flow and heat transfer over a permeable stretching/shrinking sheet with heat source effect", *International Journal of Numerical Methods for Heat & Fluid Flow*, **28**(11), pp. 2650-2663 (2018).
22. Yasin, M.H.H., Ishak, A., and Pop, I. "MHD stagnation-point flow and heat transfer with effects of viscous dissipation, Joule heating and partial velocity slip", *Scientific Reports,* **5**, pp. 17848 (2015).
23. Shateyi, S., and Makinde, O.D. "Hydromagnetic stagnation-point flow towards a radially stretching convectively heated disk", *Mathematical Problems in Engineering,* **2013**, Article ID 616947 (2013).
24. Khan, M. I., Khan, W. A., Waqas, M. et al. "Numerical simulation for MHD Darcy-Forchheimer three-dimensional stagnation point flow by a rotating disk with activation energy and partial slip", *Applied Nanoscience,* **10,** pp. 5469-5477 (2020).
25. Chu, Y.M., Khan, M. I., Rehman, M. I. U. et al. "Stability analysis and modeling for the three-dimensional Darcy-Forchheimer stagnation point nanofluid flow towards a moving surface", *Applied Mathematics and Mechanics*, **42**, pp. 357-370 (2021).

26. Chu, Y. M., Ikram, M. D., Asjad, M. I. et al. “Ghaemi. Influence of hybrid nanofluids and heat generation on coupled heat and mass transfer flow of a viscous fluid with novel fractional derivative”, *Journal of Thermal Analysis and Calorimetry,* **144**, pp. 2057-2077 (2021).
27. Mustafa, I., Javed, T., and Ghaffari, A. “Heat transfer in MHD stagnation point flow of a ferrofluid over a stretchable rotating disk”, *Journal of Molecular Liquids,* **219**, pp. 526-532 (2016).
28. Roşca, N.C., and Pop, I. “Axisymmetric rotational stagnation point flow impinging radially a permeable stretching/shrinking surface in a nanofluid using Tiwari and Das model”, *Scientific Reports,* **7,** Article ID 40299 (2017).
29. Abbasi, A., Gulzar, S., Mabood, F. et al. “Nonlinear thermal radiation and activation energy features in axisymmetric rotational stagnation point flow of hybrid nanofluid”, *International Communications in Heat and Mass Transfer,* **126**, Article ID 105335 (2021).
30. Farooq, W., Abbasi, A., Al- Khaled, K. et al. “Thermal aspect of boron nitride nanotubes (BNNT) and multiwall carbon nanotubes (MWCNT) with distinct physical features: Keller Box simulations”, *ZAMM- Journal of Applied Mathematics and Mechanics/Zeitschrift für Angewandte Mathematik und Mechanik,* **102**(10), Article ID e202100560 (2022).
31. Rivlin, R.S. “The hydrodynamics of non-Newtonian fluids”, I. Proceedings of the Royal Society of London, Series A. *Mathematical and Physical Sciences,* **193**, pp. 260-281 (1948).
32. Beard, D.W., and Walters, K. “Elastico-viscous boundary-layer flows”, I. Two-dimensional flow near a stagnation point. In Mathematical Proceedings of the Cambridge Philosophical Society, *Cambridge University Press,* **60,** pp. 667-674 (1964).

33. Ariel, P.D. “A numerical algorithm for computing the stagnation point flow of a second grade fluid with/without suction”, *Journal of Computational and Applied Mathematics*, **59**(1), pp. 9-24 (1995).
34. Barış, S., and Dokuz, M.S. “Three-dimensional stagnation point flow of a second grade fluid towards a moving plate”, *International Journal of Engineering Science*, **44**(1-2), pp. 49-58 (2006).
35. Labropulu, F., Xu, X., and Chinichian, M. “Unsteady stagnation-point flow of a non-Newtonian second grade fluid”, *International Journal of Mathematical Sciences*, **2003**, Article ID 237413 (2003).
36. Bhuvaneswari, B., Eswaramoorthi, S., Sivasankaran, S., et al. “Effects of viscous dissipation and convective heating on convection flow of a second-grade liquid over a stretching surface: An analytical and numerical study”, *Scientia Iranica*, **26**(3), pp. 1350-1357 (2019).
37. Krishna, M.V., Ahamad, N.A., and Chamkha, A.J. “Hall and ion slip impacts on unsteady MHD convective rotating flow of heat generating/absorbing second grade fluid”, *Alexandria Engineering Journal*, **60**(1), pp. 845-858 (2021).
38. Xia, W., Animasaun, I.L., Wakif, A., et al. “Gear-generalized differential quadrature analysis of oscillatory convective Taylor-Couette flows of second-grade fluids subject to Lorentz and Darcy-Forchheimer quadratic drag forces”, *International Communications in Heat and Mass Transfer*, **126**, Article ID 105395 (2021).
39. Siddique, I., Tlili, I., Bukhari, S. M., et al. “Heat transfer analysis in convective flows of fractional second grade fluids with Caputo-Fabrizio and Atangana-Baleanu derivative subject to Newtonion heating”, *Mechanics of Time-Dependent Materials*, **25**, pp. 291-311 (2021).

40. Mabood, F., Tlili, I., and Shafiq, A. “Features of inclined magnetohydrodynamics on a second- grade fluid impinging on vertical stretching cylinder with suction and Newtonian heating”, *Mathematical Methods in the Applied Sciences,* (2020) https://doi.org/10.1002/mma.6489
41. Chu, Y. M., Rehman, M. I. U., Khan, M.I., et al. “Transportation of heat and mass transport in hydromagnetic stagnation point flow of Carreau nanomaterial: Dual simulations through Runge-Kutta Fehlberg technique”, *International Communications in Heat and Mass Transfer*, **118**, Article ID 104858 (2020).
42. Zhao, T., Khan, M.R., Chu, Y.M., et al. “Entropy generation approach with heat and mass transfer in magnetohydrodynamic stagnation point flow of a tangent hyperbolic nanofluid”, *Applied Mathematics and Mechanics*, **42**, pp. 1205-1218 (2021).
43. Abbas, N., Nadeem, S., Saleem, A., et al. “Analysis of non-Newtonian fluid with phase flow model”, *Scientia Iranica,* **28**(6), pp. 3743-3752 (2021).
44. Yavuz, M., Sene, N., and Yıldız, M. “Analysis of the influences of parameters in the fractional second-grade fluid dynamics”, *Mathematics*, **10**(7), Article ID 1125 (2022).
45. Nadeem, M., Siddique, I., Awrejcewicz, J., et al. “Numerical analysis of a second-grade fuzzy hybrid nanofluid flow and heat transfer over a permeable stretching/shrinking sheet”, *Scientific Reports,* **12**, Article ID 1631 (2022).
46. Nisa, Z.U., Shah, N.A., Tlili, I., et al. “Natural convection flow of second grade fluid with thermal radiation and damped thermal flux between vertical channels”, *Alexandria Engineering Journal,* **58**(4), pp. 1119-1125 (2019).
47. Alamri, S. Z., Khan, A. A., Azeez, M., et al. “Effects of mass transfer on MHD second grade fluid towards stretching cylinder: a novel perspective of Cattaneo-Christov heat flux model”, *Physics Letters A*, **383**(2-3), pp. 276-281 (2019).

48. Khan, A. A., Naeem, S., Ellahi, R., et al. “Dufour and Soret effects on Darcy-Forchheimer flow of second-grade fluid with the variable magnetic field and thermal conductivity”, *International Journal of Numerical Methods for Heat & Fluid Flow*, **30**(9), pp. 4331-4347 (2020).
49. Saif, R.S., Hayat, T., Ellahi, R. et al. “Stagnation-point flow of second grade nanofluid towards a nonlinear stretching surface with variable thickness”, *Results in Physics*, **7**, pp. 2821-2830 (2017).
50. Tariq, H., Khan, A. A., and Shah, S. “Study of peristaltic transport of a dusty second-grade fluid in a curved configuration”, *Scientia Iranica*, (2023) DOI: 10.24200/SCI.2023.59041.6035
51. Dunn, J.E., and Fosdick, R.L. “Thermodynamics, stability, and boundedness of fluids of complexity and fluids of second grade”, *Archive for Rational Mechanics and Analysis*, **56**, pp. 191-252 (1974).
52. Weidman, P. “Axisymmetric rotational stagnation-point flow impinging on a rotating disk’, *Zeitschrift für angewandte Mathematik und Physik*, **66**, pp. 3425-3431 (2015).
53. Lok, Y.Y., Merkin, J.H., and Pop, I. “Axisymmetric rotational stagnation-point flow impinging on a permeable stretching/shrinking rotating disk”, *European Journal of Mechanics-B/Fluids*, **72,** pp. 275-292 (2018).

Figure Captions

Fig. 1: Geometry of the problem.

Fig. 2. Variation of radial velocity $f'(\eta)$ with We when $\sigma = 0.1$ and $S = 5.0$.

Fig. 3. Variation of swirl velocity $g(\eta)$ with We when $\sigma = 0.1$ and $S = 0.2$.

Fig. 4. Variation of radial velocity $f'(\eta)$ with σ when $We = 2.0$ and $S = 0.2$.

Fig. 5. Variation of swirl velocity $g(\eta)$ with σ when $We = 2.0$ and $S = 0.1$.

Fig. 6. Variation of radial velocity $f'(\eta)$ with S when $We = 2.0$ and $\sigma = 0.2$.

Fig. 7. Variation of swirl velocity $g(\eta)$ with S when $We = 2.0$ and $\sigma = 0.2$.

Fig. 8. Variation of temperature profile $\theta(\eta)$ with We when $S = 0.2 = \sigma$ and $Pr = 4.0$.

Fig. 9. Variation of temperature profile $\theta(\eta)$ with σ when $We = 2.0, S = 0.2$ and $Pr = 4.0$.

Fig. 10. Variation of temperature profile $\theta(\eta)$ with Pr when $We = 2.0, S = 0.2$ and $\sigma = 0.5$.

Table Captions

Table 1: Convergence of $f''(0), g''(0)$ and $-\theta'(0)$ for various number at grid points when $We = 0.1, \sigma = 1.0, Pr = 4.0, S = 0.1$ and $\beta = 0.0$.

Table 2: Comparison of $f''(0)$ and $g'(0)$ when $S = \beta = 0$ and $We = 0$.

Table 3: Variation of radial and swirl skin frictions against rotational parameter with $\beta = 0.5$ and $S = 0.1$.

Table 4: Variation of axial and swirl skin frictions against stretching parameter with $\sigma = 0.5$ and $S = 0.1$.

Table 5: Variation of Nusselt's number against rotation parameter and stretching parameter with $S = 0.1$. and $Pr = 4.0$.

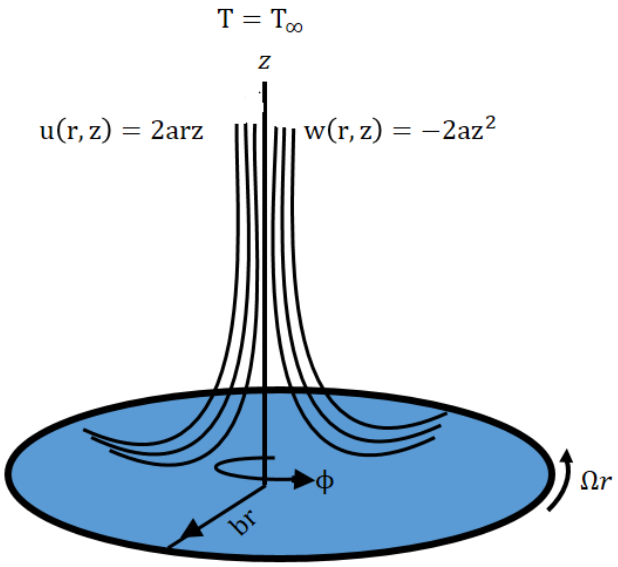

Fig. 1: Geometry of the problem.

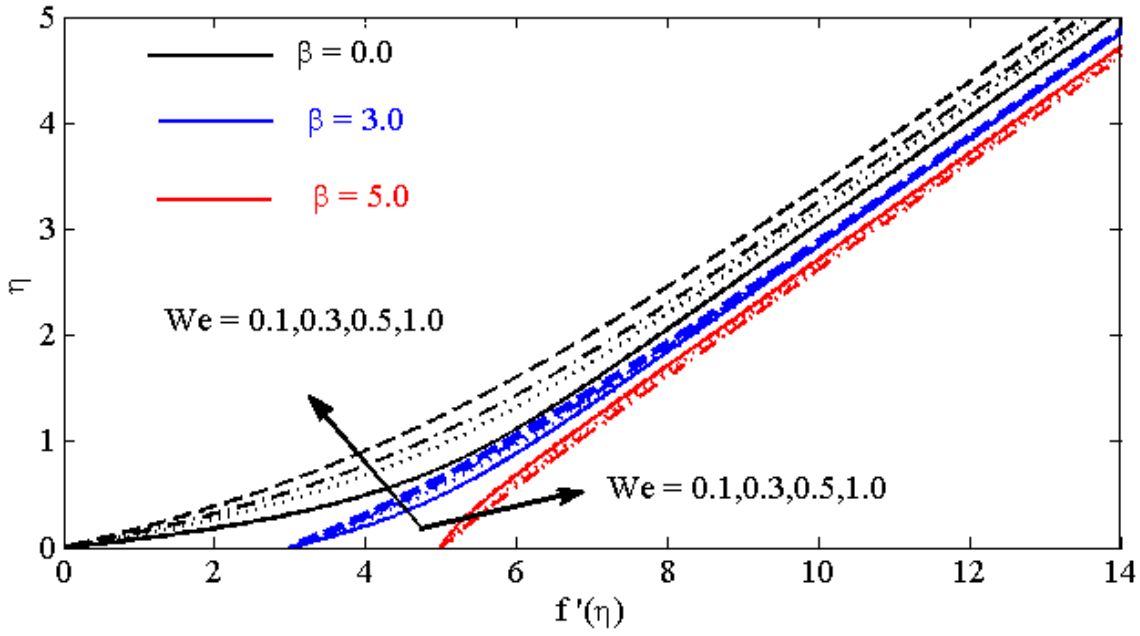

Fig. 2. Variation of radial velocity $f'(\eta)$ with *We* when $\sigma = 0.1$ and $S = 5.0$.

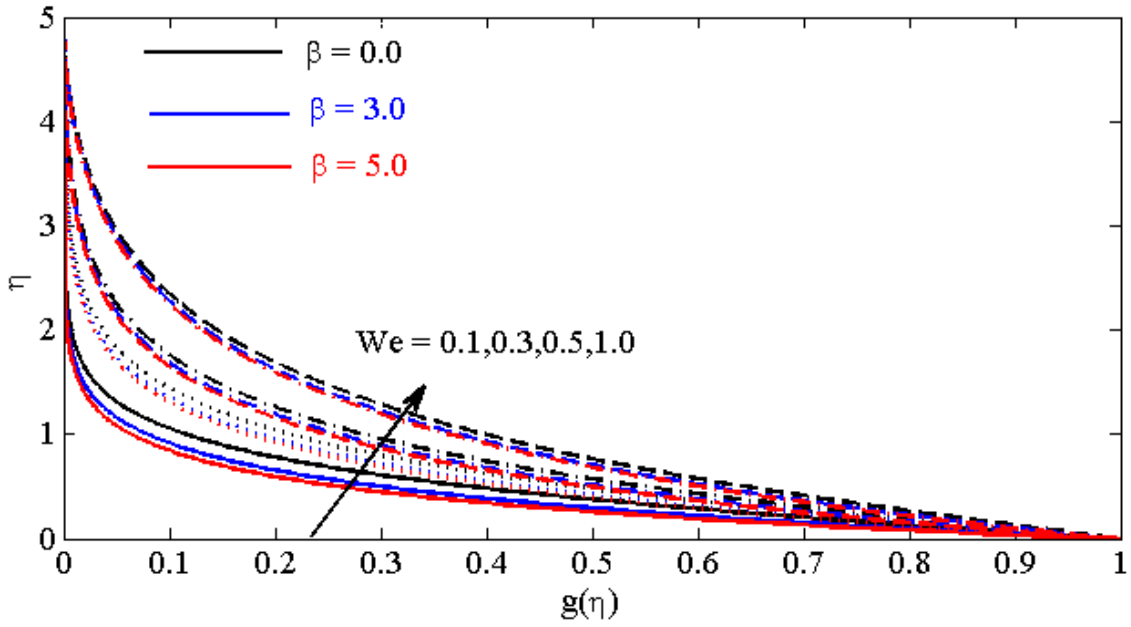

Fig. 3. Variation of swirl velocity $g(\eta)$ with We when $\sigma = 0.1$ and $S = 0.2$.

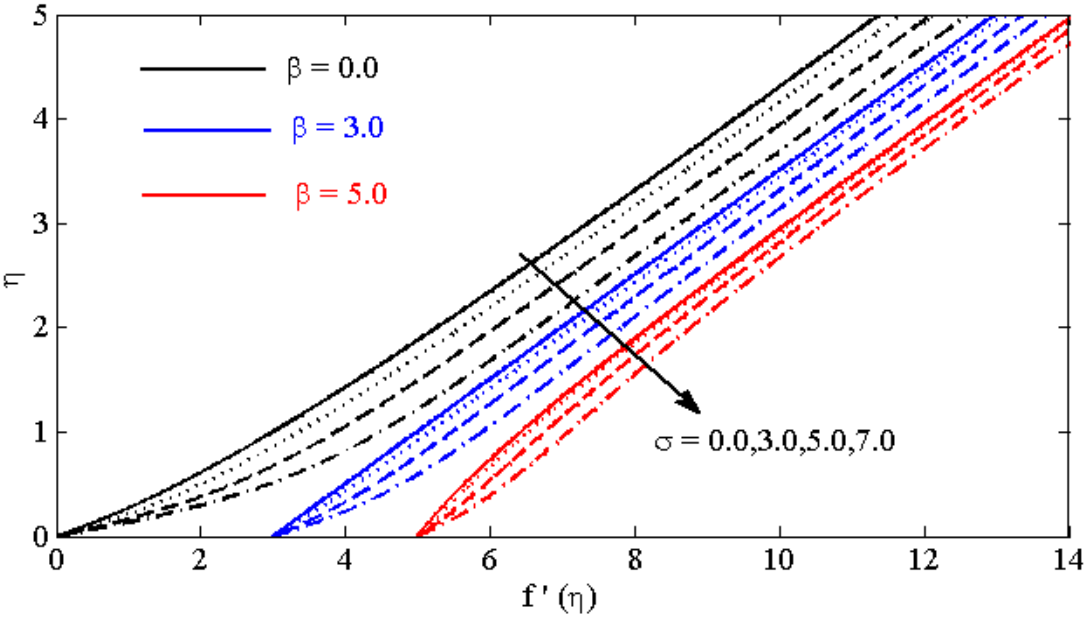

Fig. 4. Variation of radial velocity $f'(\eta)$ with σ when $We = 2.0$ and $S = 0.2$.

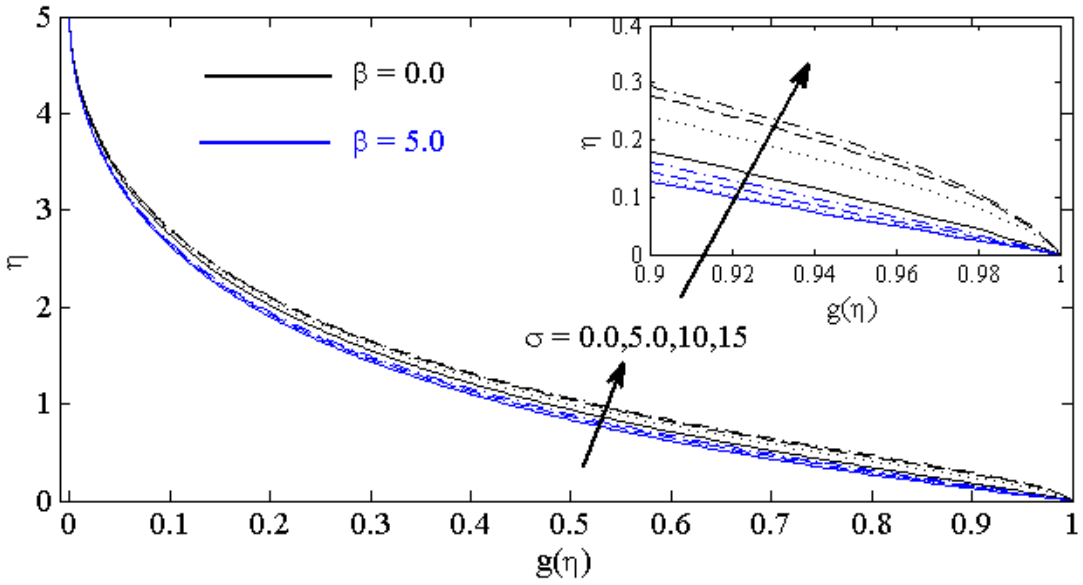

Fig. 5. Variation of swirl velocity $g(\eta)$ with σ when $We = 2.0$ and $S = 0.1$.

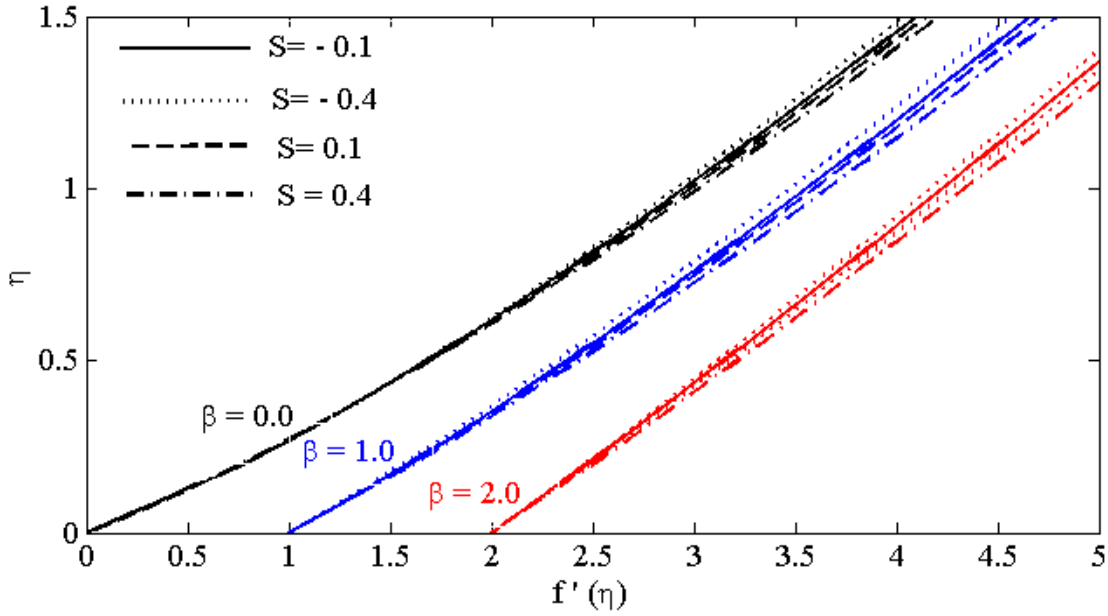

Fig. 6. Variation of radial velocity $f'(\eta)$ with S when $We = 2.0$ and $\sigma = 0.2$.

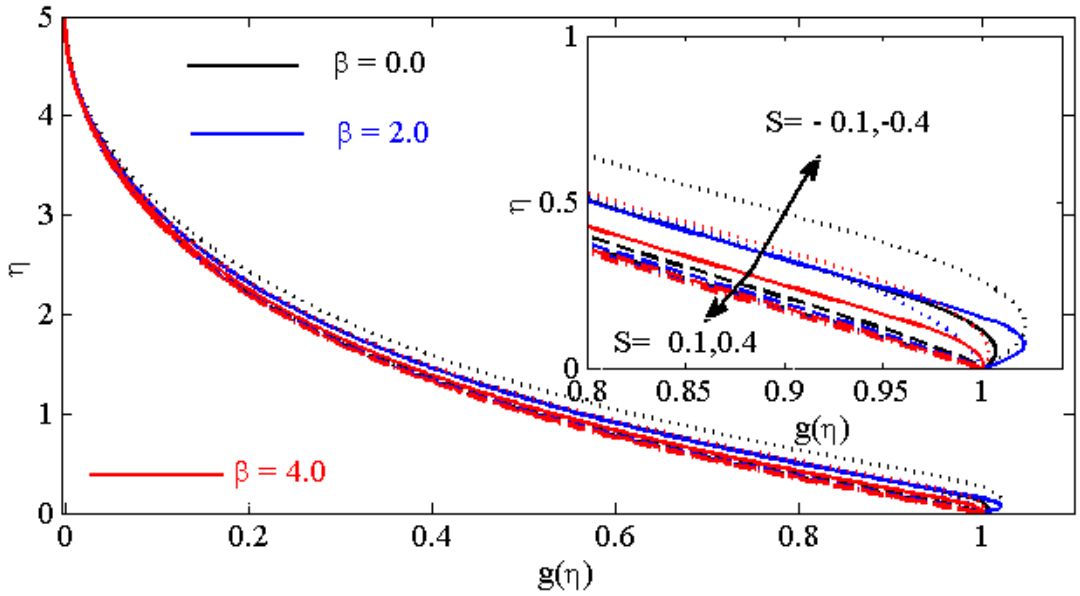

Fig. 7. Variation of swirl velocity $g(\eta)$ with S when $We = 2.0$ and $\sigma = 0.2$.

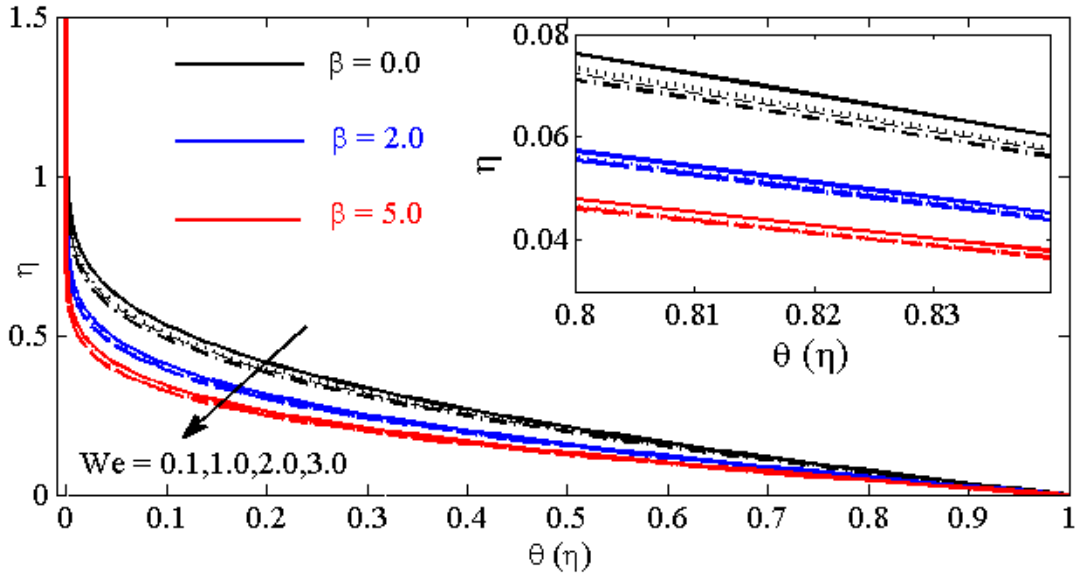

Fig. 8. Variation of temperature profile $\theta(\eta)$ with We when $S = 0.2 = \sigma$ and $Pr = 4.0$.

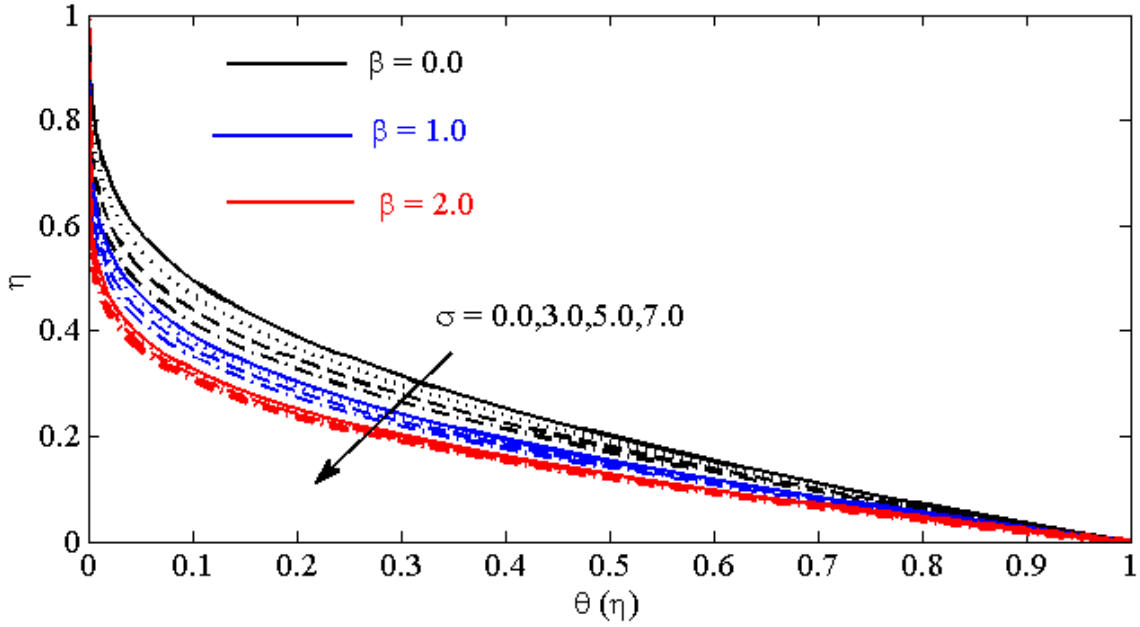

Fig. 9. Variation of temperature profile $\theta(\eta)$ with σ when $We = 2.0, S = 0.2$ and $Pr = 4.0$.

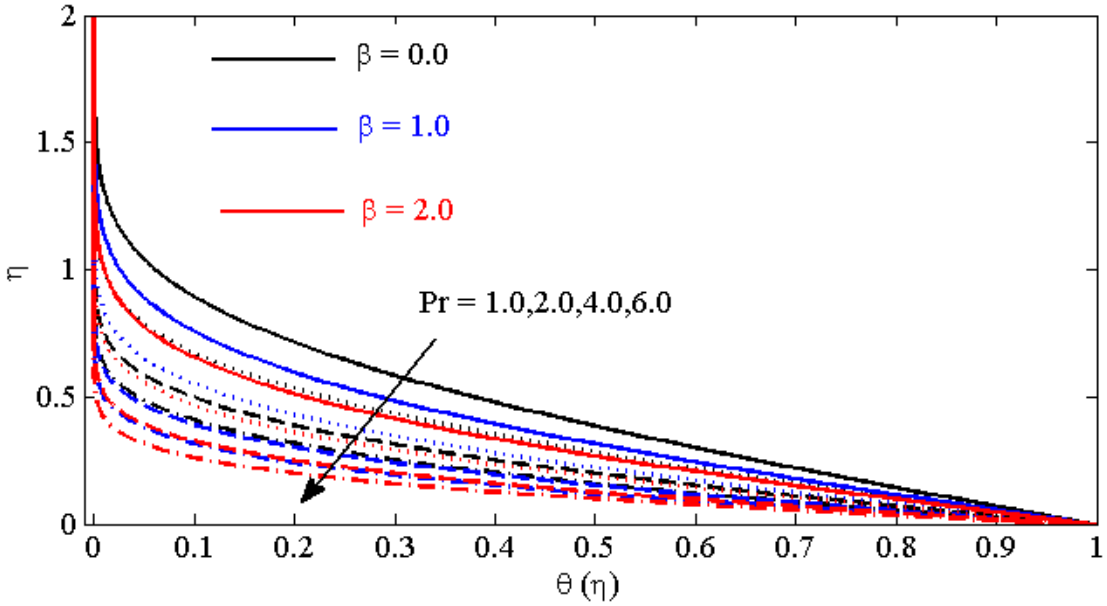

Fig. 10. Variation of temperature profile $\theta(\eta)$ with Pr when $We = 2.0, S = 0.2$ and $\sigma = 0.5$.

Table 1: Convergence of $f''(0), g''(0)$ and $-\theta'(0)$ for various number at grid points when $We = 0.1, \sigma = 1.0, Pr = 4.0, S = 0.1$ and $\beta = 0.0$.

Grid points	$f''(0)$	$g''(0)$	$f''(0)$
200	3.1363328	-1.4013549	2.2212672
400	3.1359176	-1.4010349	2.220381
500	3.1358678	1.4009965	2.2202746
1000	3.1358014	-1.4009452	2.2201328
2000	3.1357848	-1.4009324	2.2200974
3000	3.1357817	-1.4009301	2.2200908
5000	3.1357801	-1.4009289	2.2200875
10000	3.1357794	-1.4009283	2.2200861
20000	3.1357793	-1.4009282	2.2200857
30000	3.1357792	-1.4009282	2.2200856
50000	3.1357792	-1.4009282	2.2200856

Table 2: Comparison of $f''(0)$ and $g'(0)$ when $S = \beta = 0$ and $We = 0$.

σ^2	$f''(0)$		$g'(0)$	
	Present	Lok et al. [53]	Present	Lok et al. [53]
0	2.000011	2.00000	-1.339197	-1.33919
25	6.819139	6.81915	-1.7080642	-1.70806
100	17.05556	17.05561	-2.167531	-2.16752
225	30.48817	30.48822	-2.5617991	-2.56178
400	46.44322	46.44340	-2.906941	-2.90692
625	64.56087	64.56092	-3.216604	-3.21660

Table 3: Variation of radial and swirl skin frictions against rotational parameter with $\beta = 0.5$ and $S = 0.1$.

σ	Radial skin friction			Swirl skin friction		
	$We = 0.0$	$We = 0.5$	$We = 1.0$	$We = 0.0$	$We = 0.5$	$We = 1.0$
0.0	2.131884	1.774703	0.782649	-1.879153	-1.363186	-1.036682
0.5	2.177293	2.131468	1.235408	-1.882072	-1.346105	-1.012119
1.0	2.312618	3.172399	2.541887	-1.890696	-1.296779	-0.941905
1.5	2.535295	4.816952	4.561773	-1.904654	-1.220392	-0.835389
2.0	2.841467	6.952039	7.103464	-1.923399	-1.124033	-0.705161

Table 4: Variation of axial and swirl skin frictions against stretching parameter with $\sigma = 0.5$ and $S = 0.1$.

β	Radial skin friction			Swirl skin friction		
	$We = 0.0$	$We = 0.5$	$We = 1.0$	$We = 0.0$	$We = 0.5$	$We = 1.0$
0.0	2.481262	4.509229	6.142849	-1.522795	-1.010654	-0.354739
0.5	2.177293	2.131468	1.235408	-1.882072	-1.346105	-1.012119
1.0	1.577820	0.447832	-2.036308	-2.176116	-1.518813	-1.274356
1.5	0.752212	-0.698510	-4.305664	-2.431099	-1.623040	-1.405607
2.0	-0.261424	-1.361850	-5.786673	-2.659341	-1.692473	-1.481461

Table 5: Variation of Nusselt's number against rotation parameter and stretching parameter with $S = 0.1$. and $Pr = 4.0$.

σ	Nusselt's number	β	Nusselt's number

	$We = 0.0$	$We = 0.5$	$We = 1.0$		$We = 0.0$	$We = 0.5$	$We = 1.0$
0.0	2.633004	2.739910	2.780009	0.0	2.130364	2.299833	2.355965
0.5	2.636729	2.746533	2.785276	0.5	2.636729	2.746532	2.785276
1.0	2.647737	2.765821	2.800629	1.0	3.051624	3.154722	3.188188
1.5	2.665551	2.796206	2.824865	1.5	3.411054	3.528017	3.560684
2.0	2.689470	2.835546	2.856293	2.0	3.732331	3.871926	3.905467

Aamar Abbasi

Aamar Abbasi is currently working as an assistant professor in the Department of Mathematics University of Azad Jammu and Kashmir. He has PhD Degree in Mathematics from the University of Azad Jammu and Kashmir. His research area is the numerical simulations of flows of Non-Newtonian fluids.

Waseh Farooq

Waseh Farooq is a Ph.D. student in the mathematics department of the University of Azad Jammu and Kashmir. He has MPhil degree in mathematics from the university. His research interests include flows of non-Newtonian flows. He has published more than 50 research articles in well reputed Journals.

Fazle Mabood

Fazle Mabood is working as a Professor at Department of Information Technology, Fanshawe College London, ON Canada. He is reviewer of <100 international journals. He has published a lot of articles in the filed of fluid mechanics. His research area include heat transfer, nanofluids, thermal energy, mass transfer, Newtonian and Non-Newtonian fluids.

Asma Tariq

Asma Tariq has done her MS from University of Azad Jammu and Kashmir, Muzaffarabad. Currently, she is teaching at Read Foundation College, Mirpur, AJK. Her research field is simulation of Newtonian and Non-Newtonian fluids. She has published three research articles.

Dr. Sabir Ali Shehzad

Dr. Sabir Ali Shehzad is working as an Associate Professor at Department of Mathematics, COMSATS University Islamabad, Sahiwal, Pakistan. He has completed his PhD in Fluid Mechanics from Quaid-I-Azam University, Islamabad, Pakistan in 2014. His main research interests are Newtonian and non-Newtonian fluids, nanofluids and heat and mass transfer

analysis. He has published >400 research articles in various high reputed international journals. He is reviewer of >100 international journals.

Irfan Anjum Badruddin

Irfan Anjum Badruddin is working as Professor at Department of Mechanical Engineering, King Khalid University, Saudi Arabia. He graduated in Mechanical Engineering in 1998 and obtained Master of Technology in 2001 . He further obtained PhD in the field of Heat Transfer from Universiti Sains Malaysia in 2007. He works in the interdisciplinary fields and his research interest includes thermofluids, renewable energy, finite element analysis and CFD.